PACS 61.46.+w; 61.43.Hv; 61.48.De; 65.20.+w; 65.80.+n; 73.63.Fg; 73.63.-b; 82.65.+r

I.A. Melnyk [1, 2], L.A. Bulavin [2], S.V. Hrapatyi [3], G.I. Dovbeshko [4], E.A. Solovyova [1], V.A. Mykhailyk [5], N.I. Lebovka [1]

MICROSTRUCTURE AND PHYSICAL PROPERTIES OF GLYCEROL DOPED BY OXIDIZED MULTIWALLED CARBON NANOTUBES

[1] *F.D. Ovcharenko Institute of Biocolloidal Chemistry of National Academy of Sciences of Ukraine*
42 Vernadskogo Blvd., Kyiv, 03142, Ukraine, E-mail: lebovka@gmail.com
[2] *National Taras Shevchenko University, Department of Physics*
2 Acad. Glushkova Pr., Kyiv, 03127, Ukraine
[3] *National Taras Shevchenko University, Institute of Biology*
2 Acad. Glushkova Pr., Kyiv, 03022, Ukraine
[4] *Institute of Physics of National Academy of Sciences of Ukraine*
46 Nauki Pr., Kyiv, 03028, Ukraine
[5] *Institute Engineering Thermophysics of National Academy of Sciences of Ukraine*
2a Zhelyabova Str, Kyiv, 03057, Ukraine

The effect of acid treatment on the structure and properties of suspensions of multiwalled carbon nanotubes (MWCNTs) in glycerol has been investigated. The concentrations of MWCNTs were within 0–2 % by weight. Suspensions were treated during 5–60 min at T = 343 K by a mixture of concentrated nitric and sulphuric acids with the volume ratio of 1:3. The degree of acid treatment influence on the structure of suspension was analyzed using methods of thermal analysis and infrared spectroscopy. Oxidation of MWCNTs could affect significantly their thermal stability and degree of destruction. The changes in the structure of MWCNT clusters in glycerol, electrical conductivity and percolation behaviour of the systems are discussed. The acid treatment is shown to cause significant decrease in conductivity of suspension and enhancement of its temperature dependence. Reduction of the length of MWCNTs after acid treatment is reported.

Keywords: *multiwalled carbon nanotubes, oxidation, glycerol suspensions, microstructure, electrical conductivity, percolation*

INTRODUCTION

Nowadays, the nanocomposites based on carbon nanotubes, dispersed in different matrix media (polymers, liquid crystals, *etc.*), attract high fundamental and industrial interests [1–3]. Such nanocomposites were already applied in ultrafast photonics, sensor and biosensor devices, ionic batteries, tissue engineering and nano-medicine [4–7]. High geometric anisotropy (the aspect ratio of carbon nanotubes, *r*, i.e., the ratio of their length to diameter, can reach 10^3–10^4) and large electrical conductivity of carbon nanotubes can result in significant increase in the electrical conductivity of composites even at very small MWCNT fillings (< 0.01–0.1 wt. %) [8, 9].

Glycerol or its mixtures with other materials are widely used as a matrix medium for carbon nanotubes. It has been demonstrated that the flow in a glycerol-water mixture filled by carbon nanotubes can induce a voltage along the direction of the flow, and it can be useful for development of sensitive flow sensors and for energy conversion [10]. The binary water-glycerol mixtures filled by single-walled carbon nanotubes (SWNTs) demonstrate promising optical limiting properties in wide temperature diapason and good resistance to optical bleaching effects [11, 12]. A new method was developed to separate a mixture of SWNTs and multi-walled carbon nanotubes (MWCNTs) by centrifugal force in a grycerol-water mixture [13]. It has been shown that composites of glycerol with plasticized-starch (GPS)/multiwalled carbon nanotubes (MWCNTs) can be used as attractive electroactive polymer materials [14]. Glycerol pretreatment of MWCNTs was used for preparation of high performance thermoplastic

starch/carboxylate MWCNTs composites [15]. Glycerol was also used as a plasticizer for preparation of MWCNTs+carboxymethyl cellulose [16] and MWCNTs + corn starch [17] composites that may be used as suitable packaging and thermoplastic materials. These nanocomposites possess high stiffness, high strength, and enhanced electrical conductivity at very low concentrations of MWCNTs [14–17]. Also, significant enhancement of electrical conductivity in glycerol doped by MWCNTs was reported [18]. MWCNTs +glycerol composites are promising as nanofluids with intriguing heat transfer enhancement performance [19–22]. Finally, glycerol is biologically safe material, which finds widespread application in food-processing industry, medicine, and biology, and it is promising to use glycerol as a matrix in biological applications of carbon nanotubes [23].

Good functionality of the glycerol-based composites and nanofluids doped by carbon nanotubes is mainly determined by their temporal stability and reproducibility of their properties [11, 12, 20]. Usually, dispersability of carbon nanotubes in most of the media is rather bad and they show high tendency to aggregation [24, 25]. The dispersability of carbon nanotubes in glycerol or in a glycerol-water mixture can be improved by introduction of appropriate surfactants [11, 12] or by chemical oxidation of carbon nanotubes [20]. The effects of oxidative treatment can reflect appearance of carboxyl and hydroxyl groups on the surface of carbon nanotubes [26] as well as the processes of "acid destruction" and shortening of carbon nanotube length [27]. The properties of oxidized carbon nanotubes can be controlled through variation of the processing conditions and application of high temperatures or supplementary ultrasonic treatment during the oxidation [26–29].

The aim of the present study was investigation of the properties of suspensions of oxidized MWCNTs in pure glycerol. The oxidative treatment of MWCNTs was done by a mixture of nitric (HNO_3) and sulphuric (H_2SO_4) acids, and comparative studies of the produced samples using thermal analysis and infrared spectroscopy were carried out. Also, the microstructure of suspensions, their electrical conductivity and percolative properties were investigated.

MATERIALS

MWCNTs, obtained by chemical vapour deposition of graphite in the gas phase with a catalyst FeAlMo0.07 (Spetsmash, Ukraine), were used as a pristine material [30]. To separate the MWCNTs from the catalyst and mineral impurities, material was treated by aqueous solutions of alkali (NaOH) and hydrochloric acid (HCl). After that, the samples were filtered to remove the excess acid and repeatedly washed by distilled water until the pH value of distilled water was reached. The residual mass concentration of mineral impurities did not exceed 1 wt. %. In the pristine state, the MWCNTs have the outer diameter $d \approx 20$–40 nm, while their length, l, varies in the range of 5 to 10 microns [31].

Glycerol, $C_3H_8O_3$ (GOST 6259-75, "Novohim" Ltd., Kharkov , Ukraine) was used as a fluidic matrix in all the experiments. Its molecular weight is 92.09, the melting point is 291.3 K and the density is 1.261 g/cm^3 (293 K). Before using, glycerol was vacuumized for 10 h at 363 K in order to remove water contaminations.

Oxidative functionalization of MWCNTs. The scheme of acid functionalization of MWCNTs is shown in Fig. 1. A mixture of concentrated nitric (HNO_3) and sulphuric (H_2SO_4) acids with the volume ratio of 1:3 was used as an oxidative medium. The pristine sample of nanotubes (NT_0, 0.3 g) was mixed with the mixture of acids (13.5 ml) at the temperature T = 343 K. To enhance dispersing, the mixture was continuously sonicated in an ultrasonic bath. Times of oxidation were 5, 30 and 60 min and the corresponding samples were labelled as NT_5, NT_{30}, and NT_{60}, respectively. After treatment, the samples were washed by distilled water and centrifuged. This procedure was repeated until reaching the constant level of pH in the supernatant (≈ 7). Then the samples were freeze-dried under vacuum for 24 h in order to obtain well flaked samples.

Preparation of MWCNTs + glycerol suspensions. The appropriate amounts of NT_0, NT_5, NT_{30} and NT_{60} were added to glycerol and the mixtures were sonicated during 10 min using an ultrasonic disperser UZDN-20/40 (Ukrprylad, Sumy, Ukraine) at the frequency of 44 kHz and the output power of 150 W. To prevent overheating of the samples, they were cooled in a water bath, so, the temperature of the samples during sonication never exceeded 323 K. The weight concentration of nanotubes in glycerol, C, was varied in the range of 0–2 wt. % Then measurements were started immediately after sonification.

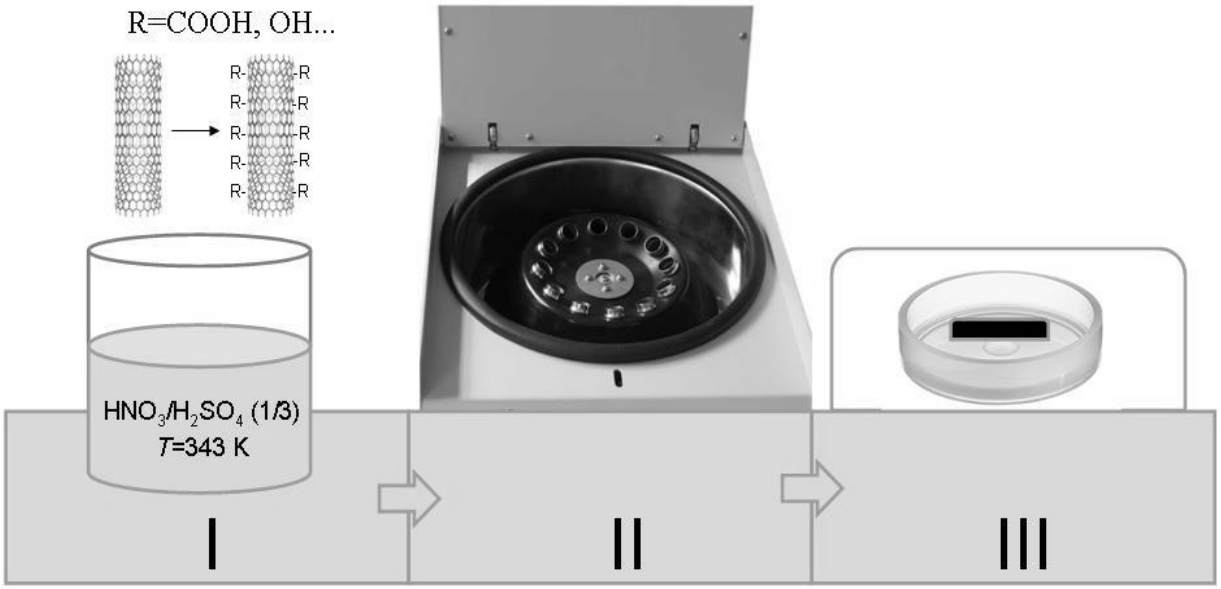

Fig. 1. Scheme of the oxidative functionalization of MWCNTs. I: acid treatment in an ultrasonic bath, II: washing and centrifugation, III: freeze-drying

METHODS

Differential thermal analysis. Differential thermal analysis of the samples NT_0, NT_5, NT_{30}, and NT_{60} was performed using a Q-1000 derivatograph (MOM, Hungary) equipped with a data logger. The study was carried out in the dynamic mode in air, in the temperature range of 293–1273 K, at the heating rate of 7.4 K/min. Samples (40 mg) were placed in a conic platinum crucible.

The reduced mass losses, m^*, were calculated as

$$m^* = \frac{m_i - m}{m_i - m_f} \qquad (1)$$

where m_i and m_f are the initial and final masses of the sample, respectively.

Infrared (IR) spectroscopy. IR spectra of samples NT_0, NT_5, NT_{30}, and NT_{60} were recorded using a Spectrum BX FT-IR instrument (Perkin Elmer, USA) in the spectral range of 4000–400 cm^{-1} with resolution of ≈ 0.8 cm^{-1}. The tablets of potassium bromide (KBr) with 0.03 wt. % nanotubes were used. The necessity in such small concentration of nanotubes was caused by high scattering and absorption capacity of MWCNTs [27].

Microstructure. Optical microphotographs of MWCNTs + glycerol suspensions were obtained using a Biolar 03–808 microscope (Warsaw, Poland) equipped with a digital camera. The suspensions were placed in a flat cell with the layer thickness of 70 μm. All measurements were done at 293 K. The microstructure of composites was characterized by analysis of the binary (black and white) images with the help of the program ImageJ v1.41. The cumulative functions of the cluster size distribution, F(r), and the average cluster size, r_m, were determined by analysis of binary images using the Hoshen-Kopelman algorithm [32] in order to identify different clusters. Fractal dimension, d_f, was calculated by counting the number of square cells needed for covering the cell perimeter, N, versus the size of the cell, L, using equation [33]:

$$N \propto L^{d_f}. \qquad (2)$$

The value of d_f reflects morphology of the two-dimensional projections.

Electrical conductivity. Electrical conductivity of MWCNTs + glycerol suspensions was measured in a flat cell with 500 μm distance between the electrodes [8] by an AM 3003 conductivity meter (Data.com, Russia) at the frequency of 1 kHz and the voltage of 0.25 V. The

choice of 1 kHz allowed avoiding of the effects of near-electrode polarization and migration of nanoparticles in electric field [34]. The temperature was varied in the heating-cooling cycles within 290–333 K at the rate of 2.0 K/min. A typical electrical conductivity hysteresis was observed: the electrical conductivity during heating was lower than that during cooling [8]. The hysteresis loops were becoming smaller with increase in the number of cycles, *N*. Such behaviour reflected the effect of restructuring of MWCNT clusters owing to their Brownian motion. In these experiments, the hysteresis loop became insignificant at $N \geq 3$, therefore, we refer in our further discussions only to the data obtained in the third cycle.

The temperature was regulated by a THERMOSTAT-T:03 water thermostat (Mechanik Pruefgeraete Medingen, Germany) and was controlled (±0.1 K) by a K-type thermocouple using a Center SE309 instrument (JDC Electronic SA, Sweden).

Statistical analysis. Each experiment was performed, at least, three times in order to determine the mean values and the mean square errors. The appropriate parameters and correlation coefficients were determined by least squares method using Table Curve 2D (Jandel Scientific, USA).

RESULTS AND DISCUSSION

Modification of the MWCNT surface by oxidative functionalization. Previous studies have shown that the time of acid treatment can significantly influence the thermal stability of MWCNTs and the patterns of their IR spectra [27, 29, 35–38]. Fig. 2 shows the temperature dependence of the reduced mass, m^* (*a*), and its temperature derivative, $-dm^*/dT$ (*b*), for the NT_0, NT_5, NT_{30}, and NT_{60} samples. The data evidence that acid treatment strongly influences thermogravimetric behaviour of the samples. The NT_0 sample started to lose its weight at 800 K, while thermal degradation of oxidized samples NT_5, NT_{30}, and NT_{60} took place at significantly lower temperatures. It was observed in the temperature range of 450 to 600 K which could reflect decarboxylation of MWCNT surface [29]. Reduction of thermal stability can evidence the presence of disordered or amorphous carbon in the oxidized samples as a result of the partial destruction of MWCNTs [35]. The derivatives $-dm^*/dT$ of all the samples NT_0, NT_5, NT_{30}, and NT_{60} passed through a maximum approximately at the same temperature, about 960 K. This temperature corresponds to the most intensive oxidation of well graphitized structures, i.e. nanotubes. The intensity of $-dm^*/dT$ peaks decreased and their half-width, ΔT, increased with increase of the time of oxidative functionalization (Fig. 2 *b*). It can indicate enhancement of destruction of the nanotubes. These data are in full accordance with the results of the previous studies of the impact of acid treatment on the thermal stability of MWCNTs [29].

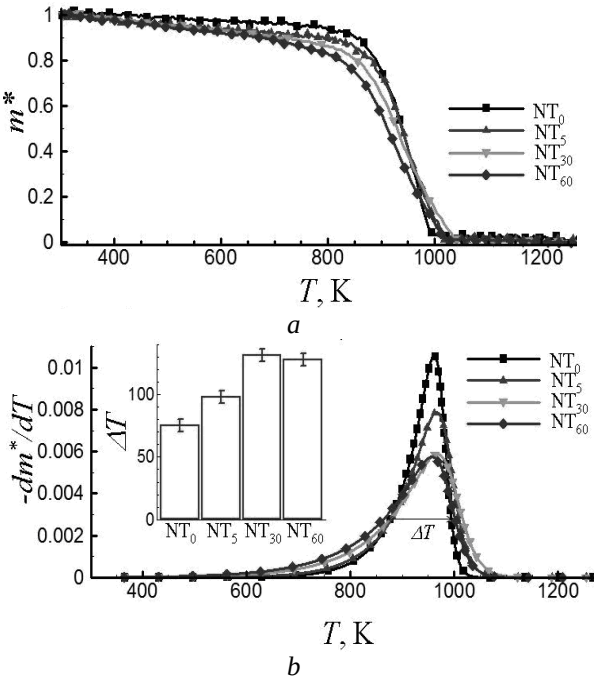

Fig. 2. Reduced mass loss, m^* (*a*), and temperature derivative, $-dm^*/dT$ (*b*), versus the temperature, *T*. The insert to (*b*) shows the half-width of peak $-dm^*/dT$ for the samples NT_0, NT_5, NT_{30}, and NT_{60}

Fig. 3 compares IR spectra of different samples NT_0, NT_5, NT_{30}, and NT_{60}. The obtained data are in correspondence with the previously reported data for impact of oxidation of MWCNTs on the chances in IR spectra [27, 36–38]. The spectra of the all samples showed a number of vibrational bands in the region of 700–4000 cm^{-1}. The main bands could be attributed to: 1) OH stretching modes in the 3200–3600 cm^{-1} with maximum near 3420 and 3460 cm^{-1}; 2) OH deformation modes near 1635 cm^{-1}, CH_2 stretching modes near 2850 and 2920 cm^{-1}, COOH in the 1680–1780 cm^{-1} region, CH_2 deformation modes near 1460 cm^{-1}, C–O C–C in the region of 1000–1300 cm^{-1} [27, 29, 36, 39, 40]. The stretching bands of

methylene groups CH_2 and C=O could be attributed to the groups localized on the defects of MWCNTs.

More intense peaks of OH and COOH groups at the MWCNT surface were registered after acid treatment. The spectral range of ≈ 3100–3400 cm^{-1} can be attributed to carboxylic acids with intermolecular hydrogen bonds, H-bonded hydroxyl groups, *etc.* The samples were heterogeneous and the more OH, C=O and less CH_2 groups were registered after oxidation.

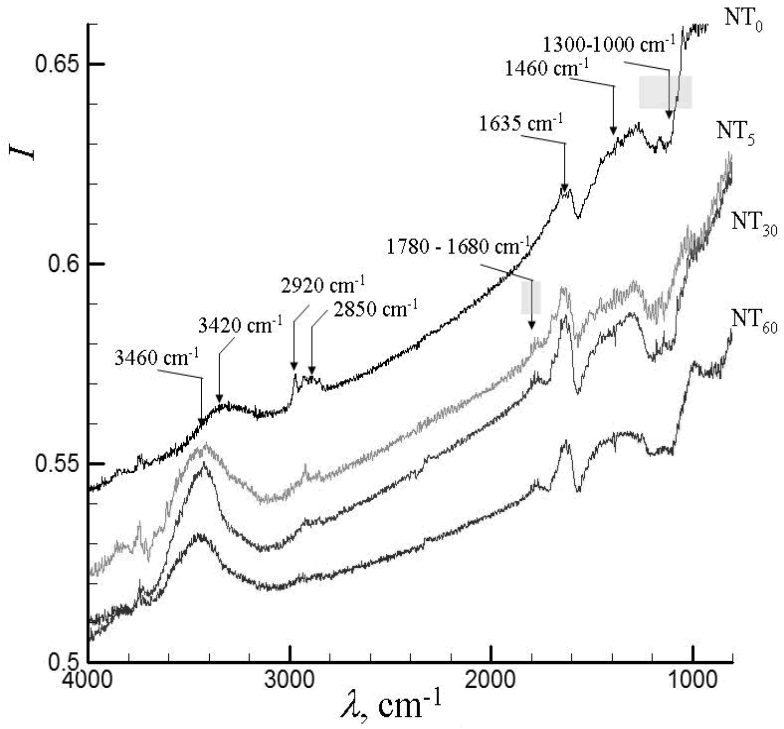

Fig. 3. IR spectra of different MWCNTs (samples NT_0, NT_5, NT_{30} and NT_{60}). T = 293 K

Microstructure of clusters in MWCNTs + glycerol suspensions. Fig. 4 shows the microphotographs of different MWCNTs + glycerol suspensions (samples NT_0, NT_5, NT_{30}, and NT_{60}) with the same concentration of MWCNTs, C = 0.05 wt. %. Significant visual changes in the size of the MWCNTs clusters dispersed in a glycerol suspension were observed with increase in the oxidation degree.

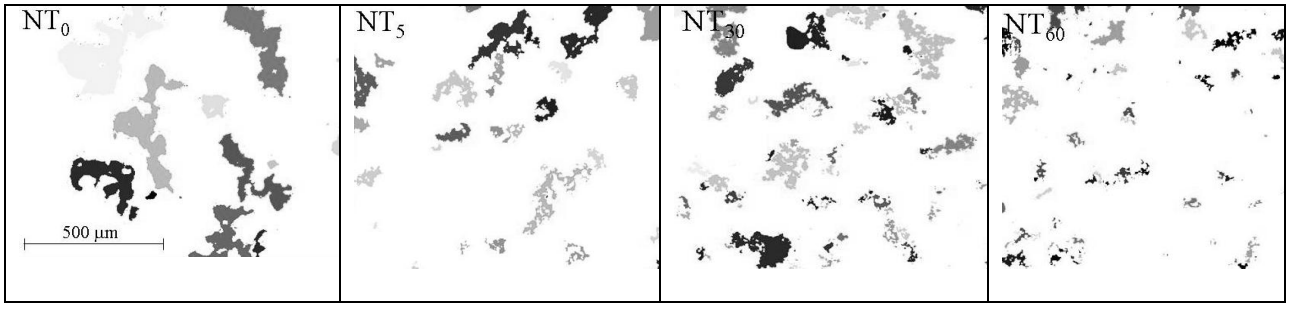

Fig. 4. Microphotographs of different MWCNTs + glycerol suspensions (samples NT_0, NT_5, NT_{30}, and NT_{60}) at the same concentration of MWCNTs, C = 0.05 wt. %. Different intensities of gray correspond to different disconnected clusters of MWCNTs identified with the help of the Hoshen-Kopelman algorithm [32]. T = 293 K

Fig. 5 shows the results of the cluster analysis. The maximum size of the cluster in NT_0 sample (pristine nanotubes) was up to 200 μm, whereas this value was noticeably smaller (≈ 70 μm) in NT_{60} sample (Fig. 5 *a*). The average radius of gyration, r_m, also decreased with increase of the time of acid treatment (Fig. 5 *b*). Additional analysis of samples with higher concentrations of MWCNTs has shown that acid treatment can also significantly affect the microstructure of clusters. The clusters had distinct fractal structure and gradually merged forming larger aggregates with increase of MWCNT concentration [18]. Black aggregates were visually recognizable on microphotographs, however, considerable part of MWCNTs was also in a well dispersed state and was invisible at optical microscopy images. Note that the ratio of MWCNTs in the aggregated and in well dispersed states can depend significantly on the concentration of MWCNTs. At certain critical concentration ($C \approx 0.1$–0.2 wt. %), the aggregates formed an infinite percolation cluster that spanned through the whole system, and above this concentration the structure of clusters was becoming more and more compact.

Fig. 6 compares microphotographs of MWCNTs + glycerol suspensions (samples NT_0 and NT_5) for two different concentrations $C = 0.2$ wt. % (*a*) and $C = 0.5$ wt. % (*b*). The visual analysis shows that acid treatment leads to formation of more compacted aggregates. Furthermore, more homogeneous structure is observed for the sample NT_0 than that for the sample NT_5 at $C = 0.5$ wt. % (Fig. 6 *b*).

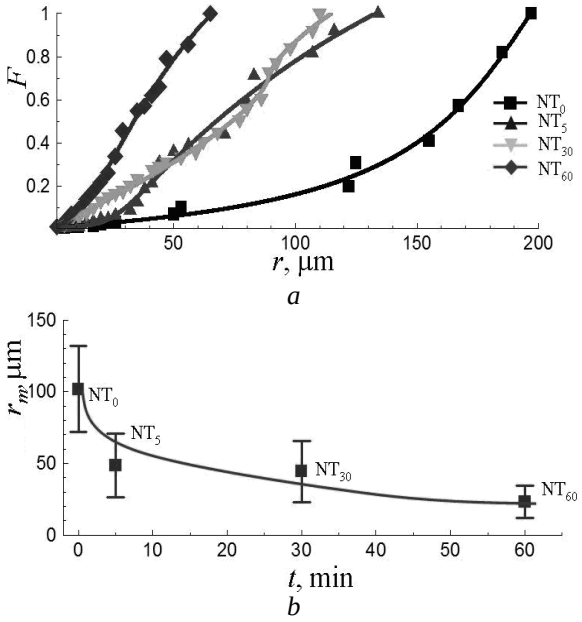

Fig. 5. Cumulative distribution function of the cluster sizes, *F(r)*, and average radius of gyration of the clusters, r_m, versus the time of acid treatment, *t*. The data obtained from analysis of the microphotographs of MWCNTs + glycerol suspensions (samples NT_0, NT_5, NT_{30}, and NT_{60}). The concentrations of MWCNTs *C* was 0.05 wt. %. $T = 293$ K

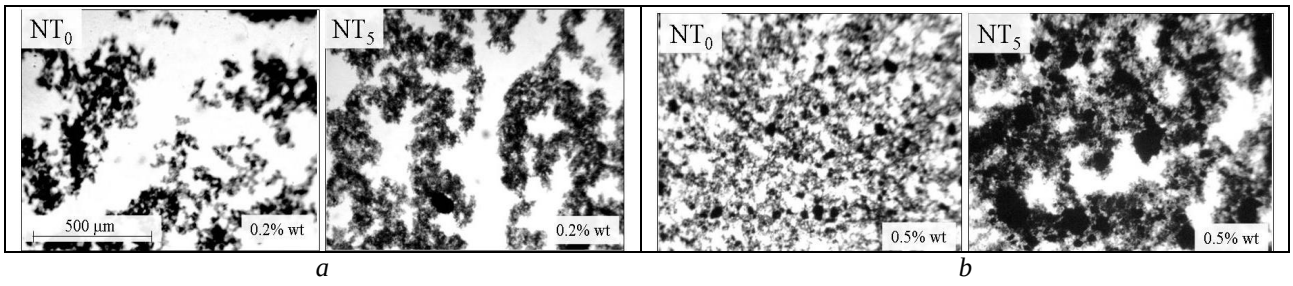

Fig. 6. Comparison of the microphotographs of MWCNTs + glycerol suspensions (samples NT_0 and NT_5) for two different concentrations of MWCNTs, $C = 0.2$ wt. % *(a)* and $C = 0.5$ wt. % *(b)*. $T = 293$ K

Fig. 7 presents the fractal dimension d_f of MWCNT aggregates versus the concentration *C* of nanotubes in samples NT_0 and NT_5. The value of d_f is characteristic for two-dimensional projections of MWCNT aggregates. It varies between 1 for linear structures and 2 for compact structures. The fractal dimension of three-dimensional aggregates can be estimated as $d^3_f = d_f + 1$ [33]. An increase in d_f with *C* increase was observed. It reflected the gradual compacting of the structure of aggregates. Moreover, the structures of aggregates seemed to be more compacted in acid-treated samples NT_5 as

compare with untreated samples NT_0 with the same value of C (Fig. 6).

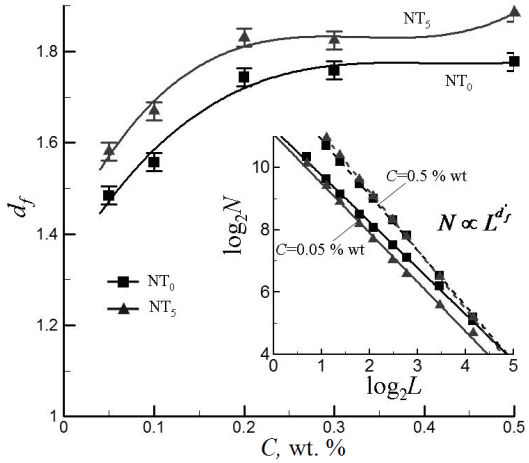

Fig. 7. Fractal dimension, d_f, of MWCNT aggregates versus concentration of MWCNTs C for MWCNTs + glycerol suspensions (samples NT_0 and NT_5). The insert shows examples of the $\log_2 N$ versus $\log_2 L$ plots for the sample NT_0 and samples with two concentrations of MWCNTs used for estimation of d_f: C = 0.05 wt. % and C = 0.5 wt. % (see Eq. 2) [31]. T = 293 K

Percolation behaviour of electrical conductivity of MWCNTs + glycerol suspensions. Fig. 8 *a* shows examples of the temperature dependences of electrical conductivity, $\sigma(T)$, for MWCNTs + glycerol suspensions (sample NT_0) at different concentrations C. Addition of MWCNTs to glycerol and increase in temperature T always resulted in increase in conductivity. A noticeable enhancement of electrical conductivity with increase of C (by several orders of magnitude) reflected a percolation transition to the more conducting state. The similar behaviour was also observed in different other suspensions filled by MWCNTs [8].

Fig. 8 *b* compares the temperature dependences of electrical conductivity $\sigma(T)$ for different samples NT_0, NT_5, NT_{30}, and NT_{60} with invariable concentration of MWCNTs, C = 0.05 wt. %. It can be seen that the acid treatment resulted in significant drop in the conductivity and changes in the character of $\sigma(T)$ dependences. The temperature dependence of $\sigma(T)$ at C = 0.05 wt. % appeared to be relatively low for the pristine sample NT_0, while significant enhancement of this dependence took place for the acid treated samples. This enhancement was clearly observed for the samples NT_5 and NT_{30}, in the whole temperature range, T = 290–340 K, while for the sample NT_{60} it was observed only at relatively high temperatures, T > 310 K (Fig. 8 *b*).

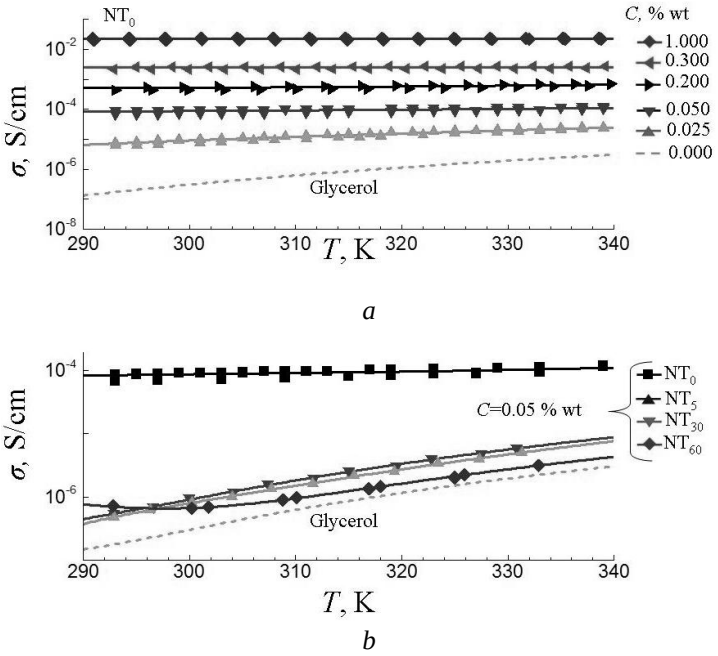

Fig. 8. Temperature dependences of electrical conductivity $\sigma(T)$ of MWCNTs + glycerol suspensions of the NT_0 samples with different concentrations of MWCNTs, C (*a*), and the same dependences for different samples NT_0, NT_5, NT_{30}, and NT_{60} with invariable concentration of MWCNTs C = 0.05 wt. % (*b*)

Note that temperature dependences $\sigma(T)$ of the studied systems (pure glycerol and MWCNTs + glycerol suspensions) followed the Arrhenius activation law only at high temperatures $T > 310$ K. Therefore, the activation energy, E, was calculated by averaging effective activation energy $E_e = d\ln\sigma/d(1/RT)$ (where R is the universal gas constant) over the temperature range of 310–340 K.

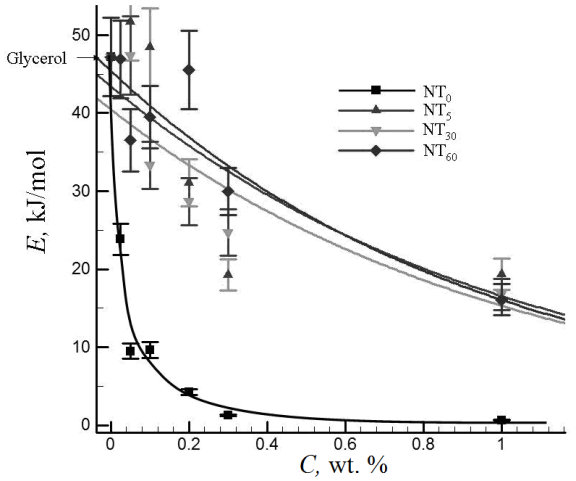

Fig. 9. Activation energy of electrical conductivity, E, versus concentration of MWCNTs, C, for the MWCNTs + glycerol suspensions (samples NT_0, NT_5, NT_{30}, and NT_{60})

Dependences of the activation energy, E, versus concentration of nanotubes, C, (samples NT_0, NT_5, NT_{30}, and NT_{60}) are presented in Fig. 9. They are characteristic of the mechanism of ionic conductivity. The value of E is decreasing with increase in C and is significantly smaller for the pristine MWCNTs (sample NT_0) than that for the acid treated MWCNTs (samples NT_5, NT_{30}, and NT_{60}). In addition, the activation energy E of the pristine MWCNTs (sample NT_0) becomes rather low above the percolation threshold ($>10^{-2}$ wt. %) and falls up to $E \approx 0$ kJ/mol at $C \geq 0.5$ wt. %. It reflects formation of a multiply connected network with numerous direct contacts between MWCNTs. At direct contacts, the electronic mechanism of electrical conductivity becomes important and ionic conductivity mechanism loses its dominant role. Such behaviour of $E(C)$ is quite typical for different nanocomposites filled by MWCNTs [31, 34]. In acid treated MWCNTs (samples NT_5, NT_{30}, and NT_{60}), the value of E remains relatively high (at the level of ≈ 20 kJ/mol) even at rather high concentrations of MWCNTs (≈ 1 wt. %) exceeding the percolation threshold. Formation of multiply connected networks of MWCNTs is visually observed in microphotographs at such concentrations. Thus, it can be assumed that oxidative functionalization of MWCNTs and covering of their surface by COOH and OH groups significantly reduce the number of direct electronic contacts between different MWCNTs, which are responsible for the electronic conductivity mechanism. The quality of electronic contact can also decrease due to introduction of numerous defects into the structure of MWCNTs, distortion of ideal graphitic structures and enhancement of the degree of carbon amorphism due to functionalization.

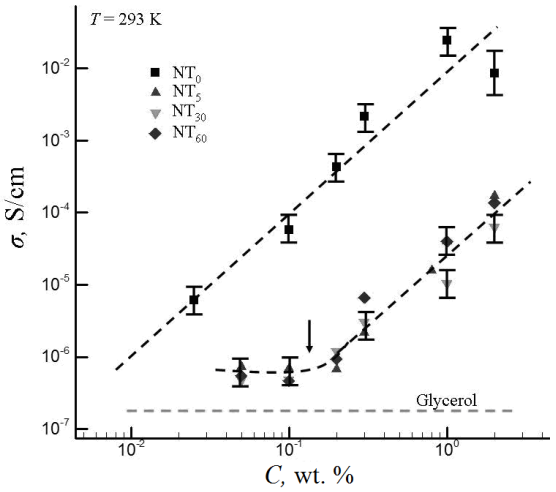

Fig. 10. Electrical conductivity, σ, versus concentration of MWCNTs, C, for the MWCNTs + glycerol suspensions (samples NT_0, NT_5, NT_{30}, and NT_{60}). T=313 K

Fig. 10 presents concentration dependences of electrical conductivity σ in MWCNTs + glycerol suspensions (samples NT_0, NT_5, NT_{30}, and NT_{60}). Analysis have shown that above the percolation threshold concentration, C_p, these dependences can be well described by the power law percolation relation [41]:

$$\sigma \propto (C - C_p)^t \qquad (3)$$

with the critical exponent $t = 1.90 \pm 0.30$ which is approximately the same for all the samples studied NT_0, NT_5, NT_{30}, and NT_{60}. Here, C_p is the percolation concentration.

The obtained value of the scaling exponent, t, is in good correspondence with the value $t \approx 2$, which is characteristic for three-dimensional random percolation problem [41]. However, it should be noted that transition from the delayed conductivity growth to the power growth of

conductivity was observed at $C \approx C_p$ = 0.2 wt. % for the acid treated samples NT_5, NT_{30}, and NT_{60}, while similar transition in the pristine sample NT_0 took place at a noticeably smaller concentration (≈ by 1 order of magnitude). Note, that the effect of percolation and formation of spanning networks in the acid treated samples NT_5, NT_{30}, and NT_{60} was visually observed at their microphotographs at $C \approx 0.2$ wt. % (Fig. 6). From the other hand, it was not visually observed at the microphotographs of pristine samples NT_0 even at $C = 0.05$ wt. % (Fig. 6), though it was expected to be above $C_p > 10^{-2}$ wt. % according to estimations made on the basis of electrical conductivity data. It may be speculated that this effect can reflect different thickness of the cells used for investigation of micrographs (70 μm) and electrical conductivity (500 μm). Note, that percolation behaviour of electrical conductivity can be rather sensible to the presence of well dispersed MWCNTs that can form invisible conductive bridges between large aggregates.

The effect of acid treatment on the percolation behaviour of suspensions filled by MWCNTs can reflect a decrease in the aspect ratio, r, of MWCNTs due to their damage and shortening. The inverse relation between the percolation concentration, C_p, and the aspect ratio is approximately fulfilled [8]

$$C_p \propto 1/r \qquad (4)$$

and the obtained data allow to conclude that acid treatment of all the samples NT_5, NT_{30}, and NT_{60} resulted in reduction of the aspect ratio, or the length of nanotubes, by about 1 order of magnitude.

CONCLUSIONS

The data obtained evidence that acidic functionalization of MWCNTs can significantly affect their thermal stability and increase the concentration of COOH and OH groups on their surfaces. The observed enhancement of thermal degradation of MWCNT suspensions at substantially lower temperatures in the case of acid treated MWCNTs evidently reflected appearance of disordered or amorphous carbon due to destruction of MWCNTs. Thermogravimetric data indicate the increase in destruction of MWCNTs with increase in the time of functionalization from 5 to 60 min. Significant visual differences in the structure and size of clusters in MWCNTs + glycerol suspensions were observed for both pristine and functionalized MWCNTs. Functionalization resulted in decrease of the cluster sizes and increase of their compactness and fractal dimension. The pronounced percolation behaviour of electrical conductivity was observed also for both pristine and functionalized MWCNTs. However, significant decrease of electrical conductivity σ and significant enhancement of its temperature dependence in MWCNTs + glycerol suspensions were exhibited by functionalized samples. The threshold concentration of percolation was estimated as ≈ 0.2 wt. %, which was approximately 1 order of magnitude higher than in pristine MWCNTs. It can reflect the decrease in the aspect ratio or the length of MWCNTs due to their damage during acidic functionalization. In general, the effects observed can be determined by several factors:

- surface functionalization of MWCNTs and increase of concentrations of COOH and OH groups on their surfaces;
- introduction of defects into the structure of MWCNTs, distortion of ideal graphitic structures and enhancement of the degree of their amorphism;
- reduction of the aspect ratio, or length, of MWCNTs due to their damage.

These factors can affect stability of suspensions, cause changes in the structure of clusters and their spatial organization, and thus influence the electrical and percolation behaviour of MWCNT suspensions.

ACKNOWLEDGEMENTS

The authors gratefully acknowledge the partial financial support of this work under project N 2.16.1.4 and number 65/14-N NAS of Ukraine. The authors also thank Dr. N.S. Pivovarova for her help with the manuscript preparation.

Мікроструктура та фізичні властивості гліцерину, легованого окисненими багатошаровими вуглецевими нанотрубками

І.А. Мельник, Л.А. Булавін, С.В. Храпатий, Г.І. Довбешко, О.О. Соловйова, В.О. Михайлик, М.І. Лебовка

Інститут біоколоїдної хімії імені Ф. Д. Овчаренка Національної академії наук України
бульв. Академіка Вернадського, 42, Київ, 03142, Україна, lebovka@gmail.com
Київський національний університет імені Тараса Шевченка, фізичний факультет
просп. Академіка Глушкова, 2, Київ, 03127, Україна
Київський національний університет імені Тараса Шевченка, інститут біології
просп. Академіка Глушкова, 2, Київ, 03022, Україна
Інститут фізики Національної академії наук України
просп. Науки, 46, Київ, 03028, Україна
Інститут технічної теплофізики Національної академії наук України
вул. Желябова, 2а, Київ, 03057, Україна

Досліджено вплив кислотної обробки на структуру та властивості суспензії багатошарових вуглецевих нанотрубок (БВНТ) в гліцерині. Концентрація БВНТ була в межах 0–2 % за масою. Суспензія була оброблена протягом 5–60 хв при T = 343 K сумішшю концентрованих азотної та сірчаної кислот в об'ємному співвідношенні 1:3. Вплив кислотної обробки на структуру суспензії аналізувався методами термічного аналізу та інфрачервоної спектроскопії. Окиснення БВНТ може істотно впливати на їхню термічну стабільність та ступінь руйнування. Обговорено зміни в структурі кластерів БВНТ в гліцерині, електропровідність та перколяційна поведінка системи. Показано, що кислотна обробка призводить до значного зменшення провідності суспензії та збільшення її температурної залежності. Одержані дані свідчать про зменшення довжини БВНТ внаслідок кислотної обробки.

Ключові слова: *багатошарові вуглецеві нанотрубки, окиснення, суспензія гліцерину, мікроструктура, електропровідність, перколяція*

Микроструктура и физические свойства глицерина, легированного окисленными многослойными углеродными нанотрубками

И.А. Мельник, Л.А. Булавин, С.В. Храпатый, Г.И. Довбешко, Е.А. Соловьева, В.А. Михайлик, Н.И. Лебовка

Институт биоколлоидной химии имени Ф.Д. Овчаренко Национальной академии наук Украины
бульв. Академика Вернадского, 42, Киев, 03142, Украина, lebovka@gmail.com
Киевский национальный университет имени Тараса Шевченко, физический факультет
просп. Академика Глушкова, 2, Киев 03127, Украина
Киевский национальный университет имени Тараса Шевченко, институт биологии
просп. Академика Глушкова, 2, Киев 03022, Украина
Институт физики Национальной академии наук Украины
просп. Науки, 46, Киев, 03028, Украина
Институт технической теплофизики Национальной академии наук Украины
ул. Желябова, 2а, Киев, 03057, Украина

Исследовано влияние кислотной обработки на структуру и свойства суспензии многослойных углеродных нанотрубок (МУНТ) в глицерине. Концентрация МУНТ находилась в пределах 0–2 % по массе. Суспензия была обработана в течение 5–60 мин при T = 343 K смесью концентрированных азотной и серной кислот в объемном соотношении 1:3. Влияние кислотной обработки на структуру

суспензии анализировалось методами термического анализа и инфракрасной спектроскопии. Окисление МУНТ может существенно влиять на их термическую стабильность и степень разрушения. Обсуждены изменения в структуре кластеров МУНТ в глицерине, электропроводность и перколяционное поведение системы. Показано, что кислотная обработка приводит к значительному уменьшению проводимости суспензии и увеличению ее температурной зависимости. Полученные данные свидетельствуют об уменьшении длины МУНТ в результате кислотной обработки.

Ключевые слова: *многослойные углеродные нанотрубки, окисление, суспензия глицерина, микроструктура, электропроводность, перколяция*

REFERENCES

1. *Pandey G., Thostenson E.T.* Carbon nanotube-based multifunctional polymer nano-composites, Polymer Reviews. 52 (2012) 355.
2. *Kovacs J.Z., Mandjarov R.E., Blisnjuk T. et al.* On the influence of nanotube properties, processing conditions and shear forces on the electrical conductivity of carbon nanotube epoxy composites, Nanotechnology, 20 (2009) 155703.
3. *Dolgov L., Kovalchuk O., Lebovka N. et al.* Liquid Crystal Dispersions of Carbon Nanotubes: Dielectric, Electro-Optical and Structural Peculiarities, in: J.M. Marulanda (Ed.), InTech, Vukovar, Croatia, 2010: pp. 451–484.
4. *Hasan T., Sun Z., Wang F. et al.* Nanotube – polymer composites for ultrafast photonics, Advanced Materials, 21 (2009) 3874.
5. *Endo M., Strano M.S., Ajayan P.M.* Potential applications of carbon nanotubes, Topics in Applied Physics, 111 (2008) 13.
6. *Harrison B.S., Atala A.* Carbon nanotube applications for tissue engineering, Biomaterials, 28 (2007) 344.
7. *Valentini F., Carbone M., Palleschi G.* Carbon nanostructured materials for applications in nano-medicine, cultural heritage, and electrochemical biosensors, Analytical and Bioanalytical Chemistry, 405 (2013) 451.
8. *Lisetski L.N., Minenko S.S., Ponevchinsky V.V. et al.* Microstructure and incubation processes in composite liquid crystalline material (5CB) filled with multiwalled carbon nanotubes, Materials Science and Engineering Technology/ Materialwissenschaft Und Werkstofftechnik, 42 (2011) 5.
9. *Pegel S., Pötschke P., Petzold G. et al.* Dispersion, agglomeration, and network formation of multiwalled carbon nanotubes in polycarbonate melts, Polymer, 49 (2008) 974.
10. *Ghosh S., Sood A.K., Kumar N.* Carbon nanotube flow sensors, Science, 299(5609) (2003) 1042.
11. *Venediktova A.V., Vlasov A.Y., Obraztsova E.D. et al.* Stability and optical limiting properties of a single wall carbon nanotubes dispersion in a binary water-glycerol solvent, Applied Physics Letters, 100 (2012) 251903.
12. *Vlasov A.Y., Venediktova A.V., Videnichev D.A. et al.* Effects of antifreezes and bundled material on the stability and optical limiting in aqueous suspensions of carbon nanotubes, Physica Status Solidi (b), 249 (2012) 2341.
13. *Yu H., Qu Y., Dong Z. et al.* Separation of mixed SWNTs and MWNTs by centrifugal force – an experimental study, in: Nano-technology, 2007. IEEE-NANO 2007. 7th IEEE Conference On, 2007: pp. 1212–1216.
14. *Ma X., Yu J., Wang N.* Glycerol plasticized-starch/multiwall carbon nanotube composites for electroactive polymers, Composites Science and Technology, 68 (2008) 268.
15. *Liu Z., Zhao L., Chen M., Yu J.* Effect of carboxylate multi-walled carbon nanotubes on the performance of thermoplastic starch nanocomposites, Carbohydrate Polymers, 83 (2011) 447.
16. *Dadfar S.M.M., Kavoosi G.* Mechanical and water binding properties of carboxymethyl cellulose/multiwalled carbon nanotube nanocomposites, Polymer Composites, 36 (2014) 7.
17. *Yurdakul H., Durukan O., Seyhan T. et al.* Microstructural characterization of corn starch-based porous thermoplastic composites filled with multiwalled carbon nanotubes, Journal of Applied Polymer Science, 127 (2013) 812.
18. *Bulavin L.A., Lebovka N.I., Kyslyi Y.A. et al.* Microstructural, rheological, and conducto-metric studies of multiwalled carbon nanotube suspensions in glycerol, Ukr. J. Phys., 55 (2010) 1.

19. *Xie H., Yu W., Li Y., Chen L.* Discussion on the thermal conductivity enhancement of nanofluids, Nanoscale Research Letters, 6 (2011) X1–12.
20. *Wang B., Lou W., Wang X., Hao J.* A gel-sol transition phenomenon of oxidation multi-walled carbon nanotubes-glycerol nanofluids induced by polyvinyl alcohol, New Journal of Chemistry, 36 (2012) 1273.
21. *Song P.C., Liu C.H., Fan S.S.* Improving the thermal conductivity of nanocomposites by increasing the length efficiency of loading carbon nanotubes, Applied Physics Letters, 88 (2006) 153111.
22. *Chen L., Xie H., Yu W., Li Y.* Rheological behaviors of nanofluids containing multi-walled carbon nanotube, Journal of Dispersion Science and Technology, 32 (2011) 550.
23. *Liu Q., Wu J., Tan T. et al.* Preparation, properties and cytotoxicity evaluation of a biodegradable polyester elastomer composite, Polymer Degradation and Stability, 94 (2009) 1427.
24. *Bergin S.D., Sun Z., Streich P. et al.* New solvents for nanotubes: Approaching the dispersibility of surfactants, Journal of Physical Chemistry C, 114 (2010) 231.
25. *Hughes J.M., Aherne D., Bergin S.D. et al.* Using solution thermodynamics to describe the dispersion of rod-like solutes: application to dispersions of carbon nanotubes in organic solvents, Nanotechnology, 23 (2012) 265604.
26. *Kahattha C., Woointranont P., Chodjarusawad T., Pecharapa W.* Study of Acid-Treated Multiwall Carbon Nanotubes by Electron Microscopy and Raman Spectroscopy, Journal of the Microscopy Society of Thailand, 24 (2010) 133.
27. *Bikiaris D., Vassiliou A., Chrissafis K., Paraskevopoulos K.M.* Effect of acid treated multi-walled carbon nanotubes on the mechanical, permeability , thermal properties and thermo-oxidative stability of isotactic polypropylene, Polymer Degradation and Stability, 93 (2008) 952.
28. *Geng H., Kim K.K., So K.P. et al.* Effect of Acid Treatment on Carbon Nanotube-Based Flexible Transparent Conducting Films, J. Am. Chem. Soc., 129(25) (2007) 7758.
29. *Datsyuk V., Kalyva M., Papagelis K. et al.* Chemical oxidation of multiwalled carbon nanotubes, Carbon, 6 (2008) 2.
30. *Melezhik A.V., Sementsov Y.I., Yanchenko V.V.* Synthesis of fine carbon nanotubes on coprecipitated metal oxide catalysts, Russian Journal of Applied Chemistry, 78(6) (2005) 917.
31. *Lebovka N., Dadakova T., Lysetskiy L. et al.* Phase transitions,intermolecular interactions and electrical conductivity behavior in carbon multiwalled nanotubes/nematic liquid crystal composites, Journal of Molecular Structure, 877 (2008) 135.
32. *Hoshen J., Kopelman R.* Percolation and cluster distribution. I. Cluster multiple labeling technique and critical concentration algorithm, Phys. Rev. B, 14 (1976) 3438.
33. *Feder J.* Fractals, Plenum Press, New York, 1988, 284p.
34. *Liu L., Yang Y., Zhang Y.* A study on the electrical conductivity of multi-walled carbon nanotube aqueous solution, Physica E, 24 (2004) 343.
35. *Hou P., Liu C., Tong Y. et al.* Purification of single-walled carbon nanotubes synthesized by the hydrogen arc-discharge method, J. Mater. Res., 16 (2001) 2526.
36. *Saleh T.A.* The influence of treatment temperature on the acidity of MWCNT oxidized by HNO_3 or a mixture of HNO_3/H_2SO_4, Applied Surface Science, 257 (2011) 7746.
37. *Scheibe B., Borowiak-Palen E., Kalenczuk R.J.* Oxidation and reduction of multiwalled carbon nanotubes: preparation and characterization, Materials Characterization, 61 (2010) 185.
38. *Shin Y.-R., Jeon I.-Y., Baek J.-B.* Stability of multi-walled carbon nanotubes in commonly used acidic media, Carbon, 50 (2012) 1465.
39. *Brichka S.Y., Prikhod'ko G.P., Sementsov Y.I. et al.* Synthesis of carbon nanotubes from a chlorine-containing precursor and their properties, Carbon, 42 (2004) 2581.
40. *Dovbeshko G.I., Gnatyuk O.P., Nazarova A.N. et al.* Vibrational Spectra of Carbonaceous Materials: A SEIRA Spectroscopy versus FTIR and Raman, Fullerenes, Nanotubes, and Carbon Nanostructures, 13 (2005) 393.
41. *Stauffer D., Aharony A.* Introduction to percolation theory, Taylor & Francis, London, 1992, 192 p.

Received 08.07.2014, accepted 26.11.2014